General Disclaimer

One or more of the Following Statements may affect this Document

- This document has been reproduced from the best copy furnished by the organizational source. It is being released in the interest of making available as much information as possible.

- This document may contain data, which exceeds the sheet parameters. It was furnished in this condition by the organizational source and is the best copy available.

- This document may contain tone-on-tone or color graphs, charts and/or pictures, which have been reproduced in black and white.

- This document is paginated as submitted by the original source.

- Portions of this document are not fully legible due to the historical nature of some of the material. However, it is the best reproduction available from the original submission.

DRA

RAY W. HERRICK LABORATORIES

A Graduate Research Facility
of The School of Mechanical Engineering

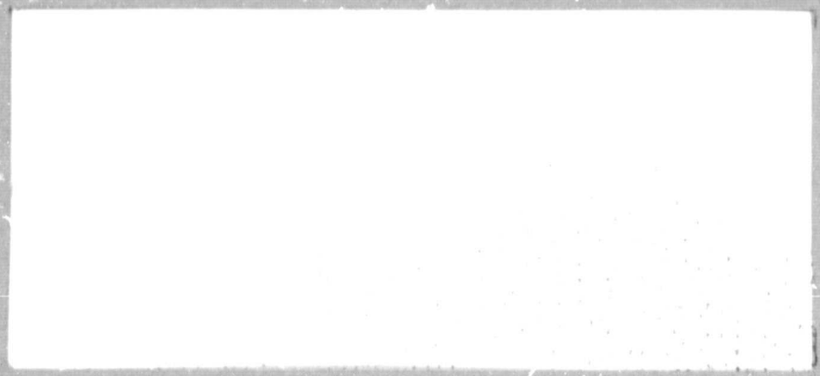

Purdue University

West Lafayette, Indiana 47907

EXPERIMENTAL DETERMINATION OF THE PARTICLE MOTIONS
ASSOCIATED WITH THE LOW ORDER ACOUSTIC MODES IN ENCLOSURES

Research Contract #0226-52-1288

EXPERIMENTAL DETERMINATION OF THE PARTICLE MOTIONS ASSOCIATED WITH THE LOW ORDER ACOUSTIC MODES IN ENCLOSURES

Sponsored by

NASA - Langley

Report NO. 5 HL 83-22

Submitted by:

Kerry P. Byrne, Visiting Scholar

Assisted by:

Steven E. Marshall, Research Assistant

Approved by:

Malcolm J. Crocker, Co-Principal Investigator
Robert J. Bernhard, Co-Principal Investigator

Approved by:

Raymond Cohen, Director
Ray W. Herrick Laboratories

July, 1983

EXPERIMENTAL DETERMINATION OF THE PARTICLE MOTIONS ASSOCIATED WITH THE LOW ORDER ACOUSTIC MODES IN ENCLOSURES

Kerry P. Byrne

School of Mechanical and Industrial Engineering,
University of New South Wales,
Kensington,
New South Wales, 2033
Australia.

Received: .....

ABSTRACT

This paper describes a procedure for experimentally determining, in terms of the particle motions, the shapes of the low order acoustic modes in enclosures. The procedure is based on finding differentiable functions which approximate the shape functions of the low order acoustic modes when these modes are defined in terms of the acoustic pressure. The differentiable approximating functions are formed from polynomials which are fitted by a least squares procedure to experimentally determined values which define the shapes of the low order acoustic modes in terms of the acoustic pressure. These experimentally determined values are found by a conventional technique in which the transfer functions, which relate the acoustic pressures at an array of points in the enclosure to the volume velocity of a fixed point source, are measured. The gradient of the function which approximates the shape of a particular mode in terms of the acoustic pressure is evaluated to give the mode shape in terms of the particle motion. The procedure was tested by using it to experimentally determine, in terms of the particle motions, the shapes of the low order acoustic modes in a small rectangular enclosure. Details of the experimental technique used and some of the results obtained are given.

INTRODUCTION

The excitation of one or more of the low order acoustic modes in an enclosure can generate in the enclosure sound pressures with distinct tonal qualities which can annoy the occupants of the enclosure. A commonly experienced example of this situation is the "cavity boom" which sometimes occurs in the cabins of passenger cars. Cavity boom arises when a low order acoustic mode, which may be coupled to a complaint portion of the enclosing structure, is excited. Usually the cavity boom is excited by the engine and it often occurs when the engine firing frequency coincides with the frequency of a low order mode. Many studies, both theoretical and experimental, have been made to investigate the low order acoustic modes in passenger cars[1,2,3]. Annoying sound pressures associated with the presence of low order acoustic modes arise in the cabins of agricultural and industrial machines[4]. A similar effect can occur in the cabins of ships and aircraft.

It is usually a simple task to experimentally determine the frequencies of the low order acoustic modes of an enclosure. However, it is not a simple task to experimentally determine the mode shapes, particularly if they vary with more than one spatial co-ordinate and if the modeshapes are required in terms of the particle motions. A knowledge of the modeshapes, and in particular the modeshapes in terms of the particle motions, is useful in devising appropriate noise control measures.

Over the last decade there have been considerable developments in experimental methods for determining the modeshapes of structures[5,6]. The ability to describe the motion of a structure when it is vibrating in a particular mode is one of the most useful developments which has occurred. The ability to describe the motion has been facilitated by the fact that a motion transducer, usually an accelerometer, is one of the two transducers

which are used to generate the electrical signals from which the transfer functions, used in the experimental modal analysis of the structure, are obtained. Although considerable developments have been made in experimental methods for determining the modeshapes of structures, it is only in recent years that attempts have been made to experimentally determine the shapes of acoustic modes[1,7,8]. One possible reason for the relative lack of progress in the acoustic case is that the most conveniently measured acoustic quantity, the acoustic pressure, cannot be used directly to determine the particle motion associated with a particular mode.

This paper describes a procedure whereby the particle motions associated with low order acoustic modes in enclosures can be derived from transfer function measurements which relate the acoustic pressures at an array of points in an enclosure to the volume velocity of a fixed point source in the enclosure. The theory of the procedure is described and then the results of a numerical evaluation of the procedure are given. Finally, a description of how the procedure was used to experimentally determine the low order acoustic modes in a small rectangular enclosure is given.

I. DESCRIPTION OF THE METHOD

Let an xyz axes system be located in the enclosure as shown in Fig. 1. The axes are not necessarily orthogonal. Suppose that LL× MM× NN transfer functions which relate the acoustic pressures at the LL× MM× NN points shown in Fig. 1 to the volume velocity of a fixed point source are measured. The points shown in Fig. I are on lines parallel to the x, y and z axes. The distances between the points on a line parallel to a particular axis need not be equal but the distances between corresponding points on different lines are equal. Suppose, that by a conventional modal analysis method, such as the method described by Nieter and Singh[8], the acoustic pressure at the point x_{II}, y_{JJ}, z_{KK} per unit volume velocity of the source is measured as $P_r(x_{II},y_{JJ},z_{KK})$ in the r^{th} mode whose angular frequency is ω_r. This measured quantity is composed of the true value, denoted $P_r^*(x_{II},y_{JJ},z_{KK})$ and an error term, denoted E. Thus:

$$P_r(x_{II},y_{JJ},z_{KK}) = P_r^*(x_{II},y_{JJ},z_{KK}) + E \qquad (1)$$

The LL× MM× NN values of $P_r(x_{II},y_{JJ},z_{KK})$ derived from the LL× MM× NN measured transfer functions can be used to determine a function which approximates $P_r^*(x,y,z)$. Let this approximating function, which is denoted $p_r(x,y,z)$, be given by:

$$\begin{aligned} p_r(x,y,z) = C(1 + X_2x + \ldots + X_Ix^{I-1} + \ldots + X_Lx^{L-1}) \times \\ (1 + Y_2y + \ldots + Y_Jy^{J-1} + \ldots + Y_My^{M-1}) \times \\ (1 + Z_2z + \ldots + Z_Kz^{K-1} + \ldots + Z_Nz^{N-1}) \end{aligned} \qquad (2)$$

The constants C,... , X_I,... , Y_J,... , Z_K,... which define the approximating function can be derived from the measured values, $P_r(x_{II},y_{JJ},z_{KK})$, by the following procedure. A total of MM× NN polynomials of the form:

$$X'_{1,JJ,KK} + X'_{2,JJ,KK}x + \ldots + X'_{I,JJ,KK}x^{I-1} + \ldots + X'_{L,JJ,KK}x^{L-1}$$

can be fitted by a least squares procedure to the LL values of $P_r(x_{II}, y_{JJ}, z_{KK})$ along each of the MM× NN lines which are parallel to the x axis. The coefficients $X'_{I,JJ,KK}$ derived from a least squares fit along a particular line can be normalized by dividing all of the coefficients by one of the coefficients. If the first coefficient is used as the normalizing coefficient, a polynomial of the following form is obtained:

$$1 + X_{2,JJ,KK}x + \ldots\ldots + X_{I,JJ,KK}x^{I-1} + \ldots\ldots + X_{L,JJ,KK}x^{L-1}$$

$X_{I,JJ,KK}$ is given by $X'_{I,JJ,KK}/X'_{1,JJ,JJ}$. Ideally, corresponding normalized coefficients for each of the MM× NN polynomials will be equal. However, since these coefficients are derived from experimental data they will differ and so X_I can be estimated by averaging the $X_{I,JJ,KK}$ coefficients. Thus X_I is given by:

$$X_I = \sum_{JJ=1}^{MM} \sum_{KK=1}^{NN} X_{I,JJ,KK} / MM \times NN$$

Along some lines parallel to the x axis the experimentally derived values $P_r(x_{II}, y_{JJ}, z_{KK})$ may be small and so the coefficients and hence the normalized coefficients may not be representative and it is prudent to discard such coefficients in the averaging. This can be done by evaluating the "size" of each of the fitted polynomials in terms of a measure such as the root mean square value of the fitted polynomial and then discarding coefficients associated with polynomials whose "size" is, for example, less than the average size.

A similar procedure involving the fitting of polynomials in the y and z directions can be used to determine the normalized coefficients $\ldots Y_J \ldots Z_K \ldots$. Once the normalized coefficients $\ldots X_I \ldots Y_J \ldots Z_K \ldots$ have been found, the coefficient C which appears in Eqn. (2) can be found to minimise the sum of the squares of the differences between $P_r(x_{II}, y_{JJ}, z_{KK})$ and $p_r(x_{II}, y_{JJ}, z_{KK})$.

It is found, in the development of the acoustic wave equation, that the acceleration of a gas particle in a particular direction is given by the negative of the gradient of the pressure in that direction divided by the density of the gas. Thus, for the r^{th} mode, the amplitude of the particle acceleration in the x direction per unit volume velocity of the source $a_{rx}(x,y,z)$, can be approximated by:

$$a_{rx}(x,y,z) \approx \frac{1}{\rho}\frac{\partial p_r(x,y,z)}{\partial x} \qquad (3)$$

It can be seen from this equation that the first partial derivative of the approximating function with respect to x must be found. This can be readily done when $p_r(x,y,z)$ is defined in the form of Eqn. (2). The amplitudes of the particle velocity and the particle displacement can be readily found from the amplitude of the acceleration. Similarly, the amplitudes of the acceleration, velocity and displacement in the y and z directions can be estimated from the partial derivatives of the approximating function with respect to y and z.

II. CALCULATIONS WITH THE FITTING PROCEDURE

It is evident that the approximating function $p_r(x,y,z)$ must approximate $p_r^*(x,y,z)$ sufficiently well so that the first partial differentials of $p_r(x,y,z)$ and $p_r^*(x,y,z)$ are in satisfactory agreement. An indication of how many terms should be incorporated in the approximating function can be obtained by using a suitable differentiable function to generate data at the points x_{II}, y_{JJ}, z_{KK}; II = 1,LL; JJ = 1,MM; KK = 1,NN, fitting approximating functions with various numbers of terms and then comparing the first partial differentials of the original and the approximating functions.

A suitable differentiable function is given by:

$$P_r^*(x,y,z) = \cos(\ell\pi x)\cos(m\pi y)\cos(n\pi z) \qquad (4)$$

$$\ell,m,n = 0,1,2,\ldots$$

This function, in addition to being readily differentiable, defines in terms of the acoustic pressure, the shapes of the modes in a rectangular enclosure whose sides have unit lengths in the x, y and z directions. There are ℓ, m and n half waves in the x, y and z directions.

Fig. 2(a) shows the values of the original and the approximating functions along the x axis after an approximating function with $L = M = N = 3$ was fitted to $LL = MM = NN = 4$ values derived from the original function, Eqn. (4), with $\ell = m = n = 1$. The gradients along this line in the x, y and z directions are shown in Fig. 2(b) for the original and the approximating functions. Figs. 3(a) and 3(b) show the corresponding results for the case of $L = M = N = 4$, $LL = MM = NN = 5$ and $\ell = m = n = 1$. Comparison of Figs. 2(b) and 3(b) indicates that if a mode in an enclosure involves a half wave in a given direction, the corresponding approximating polynomial should incorporate at least four coefficients. It is of interest that, for a rectangular enclosure, seven modes can occur when there is no more than one half wave in each of the x, y and z directions.

Fig. 4(a) shows the values of the original and approximating functions along the x axis after an approximating function with $L = M = N = 6$ was fitted to $LL = MM = NN = 7$ values derived from the original function, Eqn. (4), with $\ell = m = n = 2$. The gradients along this line in the x, y and z directions are shown in Fig. 4(b), for the original and the approximating functions. Figs. 5(a) and 5(b) show the corresponding results for the case of $L = M = N = 7$, $LL = MM = NN = 8$ and $\ell = m = n = 2$. Comparison of Figs. 4(b) and 5(b) indicates that if a mode in an enclosure involves two half waves in a given direction, the corresponding approximating polynomial should incorporate at least seven coefficients.

It is of interest, that, for a rectangular enclosure, fifteen modes can occur when there are no more than two half waves in each of the x, y and z directions.

Although it is possible to fit polynomials to modes which involve more than two half waves in each direction, the number of coefficients required in the approximating polynomial becomes large as does the number of points at which measurements must be made. The number of data points at which measurements must be made depends upon the magnitude of the error term E in Eqn. (1) relative to the magnitude of the true value of the function. If more than two half waves occur in a given direction, the approximating function can be fully or partially constructed from harmonic functions instead of the polynomials used in Eqn. (2).

III. EXPERIMENTS

The previously described procedure was applied to experimentally determining the shapes of the particle velocity modes in a small rectangular enclosure. These modeshapes can be compared with the theoretically determined modeshapes.

The internal dimensions of the rectangular enclosure and the orientation of the xyz axes system are shown in Fig. 6. The acoustic field in the enclosure was excited by a horn driver which was located in the $x = 0$, $y = 0$, $z = L_z$ corner of the enclosure. The horn driver, which was driven by noise which was white over the 50 Hz to 500Hz range contained a microphone in the magnet cavity so that the volume velocity of the source could be measured. Details of the source and how it was calibrated are given in Appendix A.

Transfer functions which related the acoustic pressures at points along lines parallel to the x, y and z axis to the volume velocity of the source were measured. The points, which were equally spaced along the lines, were defined by the values LL= 11, MM =7 and NN =9. The values of $P_r(x_{II}, y_{JJ}, z_{KK})$ were determined for the first ten resonance frequencies by the coincident-quadrature procedure[6]. An approximating function was fitted to each of the ten sets of data by the previously described procedure. First, all of the sets were fitted with polynomials defined by L= M= N= 6 so that the general shape of the mode in the direction of each axis could be estimated. The appropriate values of the polynomials in each direction for each set of data could then be fixed. If there were two half waves in a given direction the polynomial index L, M or N for that direction was set to 7 on the basis of the results given in the previous section. If there was one half wave in a given direction, the polynomial index L, M or N for that direction was set to 4. If the acoustic pressure amplitude was nominally constant in a given direction, the polynomial index L, M or N for that direction was set to 2.

A sample of the results derived is presented in Figs. 7 and 8. The results given in Fig. 7 relate to the first mode, whose frequency was 123.8 Hz. It was found, with reference to Fig. 6, that there was one half wave in the x direction and no variaition in the y and z directions. The amplitude of the acoustic pressure per unit volume velocity of the source varied along the x axis as shown in Fig. 7(a). Values derived from the approximating function and from the measurements along a line close to the axis are shown. The particle velocities derived from the approximating function varied along the x axis as shown in Fig. 7(b). The results given in Fig. 8 relate to the tenth mode whose frequency was 302.8 Hz. It was found, with reference to Fig. 6, that for this mode, there were two half waves in the x direction, one in the y direction and there was no variation

in the z direction. The ninth mode, which involved two half waves in the z direction and no variation in the x and y directions occurred at a frequency of 296.2 Hz, only 2% lower than the frequency of the tenth mode. The amplitudes of the acoustic pressure per unit volume velocity of the source varied along the x and y axes as shown in Figs. 8(a) and 8(b). Values derived from the approximating function and from the measurements along lines close to these axes are shown. The particle velocities derived from the approximating function are shown in Figs. 8(c) and 8(d).

Although the results given in Figs. 7(b), 8(c) and 8(d) contain the expected features of themodeshapes in terms of the particle motions, they do not exhibit the expected results at the boundaries. Thus, for example, in Fig. 7(b), it can be seen that although the particle velocity in the x direction is zero at $x = 0$, it is not zero at $x = 1.482$ m. This feature was found to be present to a lesser extent in the corresponding results for other modes. This situation is probably due to a number of factors such as the non-rigid boundary of the enclosure used in the experiments and the irregular data which defined the shapes of the modes in terms of the acoustic pressure. A comparison of Figs. 7(a) and 8(a) shows that the experimental data for the first mode was in general more irregular than that for the tenth mode. However, if it is certain that a particular boundary is rigid, the least squares fitting procedure can be readily modified to make the gradient of the approximating function at and normal to that boundary zero. The particle velocity at and normal to that boundary will then be zero.

IV. CONCLUDING REMARKS

The experimental results derived from the procedure described in this paper suggest that the procedure can be developed to allow the particle motions associated with low order acoustic modes in enclosures to be found. The possibility of displaying these modes in animated form as is presently done in displaying the vibrational modes of a structure then exists. Undoubtedly, superior approximating functions than the one defined by Eqn. (2) exist and several types of approximating functions are currently being investigated.

Particular attention is being paid to the ability of these approximating functions to extract useful information from irregular data. However, the approximating function defined by Eqn. (2) can be rapidly determined with basic computational facilities, a feature not possessed by other approximating functions which were considered.

REFERENCES

1. D.L. Smith, "Experimental Techniques for Acoustic Modal Analysis of Cavities", INTER-NOISE 76 Proc., 129-132 (1976).

2. D.J. Nelske and L.J. Howell, "Automobile Interior Noise Reduction Using Finite Element Methods", SAE Paper 780365 (1978).

3. L.J. Howell, "An Overview of Structures and Acoustics Technology in Automotive Applications", SAE Paper 800611 (1980).

4. G.H. Koopmann and H.H. Benner, "Noise Reduction in Tractor Cabs", INTER-NOISE 78 Proc., 353-358 (1987).

5. M. Rades, "Methods for the Analysis of Structural Frequency-Response Measurement Data", Shock Vib. Dig., 8 (2) 73-88 (1976).

6. M. Rades, "Analysis Techniques of Experimental Frequency Response Data", Shock Vib. Dig., 11(2), 15-24 (1979).

7. C.J. Moore, "Measurement of Radial and Circumferential Modes in Annular and Circumferential Fan Ducts", J. Sound Vib., 62(2), 235-256 (1979).

8. J.J. Nieter and R. Singh, "Acoustic Modal Analysis Experiment", J. Acoust. Soc. Am., 72(2), 319-326 (1982).

APPENDIX A

THE CALIBRATED VOLUME VELOCITY SOURCE

The calibrated volume velocity source was constructed from the driver of a horn type loudspeaker. The horn driver was modified by grinding slits into the magnet so that the volume between the diaphragm and the magnet was freely connected to the volume around the magnet. Pressure changes in the volume around the magnet due to the motion of the diaphragm of the driver could be measured by a microphone which was inserted into the volume around the magnet. A cross-section of the arrangement is shown in Fig. A.1. Thus by measuring the pressure with the microphone, the volume velocity produced by the source could be determined.

It can be easily shown that, if the total volume enclosed by the diaphragm, V_o , changes by a small amount, δV, the absolute pressure, P_o , in this volume changes by a small amount, $\delta P = -\delta V \times (\gamma P_o / V_o)$, if the gas in the volume behaves in an adiabatic manner. The specific heats ratio is given by γ. Thus the volume velocity $U(t)$ of the source is related to the acoustic pressure $p(t)$ in the volume behind the diaphragm by Eqn. (A.1):

$$U(t) = -(V_o/\gamma P_o) \times dp(t)/dt \qquad \text{(A.1)}$$

The volume enclosed by the diaphragm, V_o , being of very irregular shape, could not be accurately determined and so the calibration was made by measuring the acoustic pressure in a small accurately known volume which was attached to the throat of the driver along with the voltage generated by the microphone which was used to measure the acoustic pressure in the volume enclosed by the diaphragm. The volume velocity was derived from the acoustic pressure measured in the small accurately known volume by use of an equation of the form of Eqn. (A.1). The amplitude of the frequency response function relating the volume velocity produced by the source and the voltage generated

by the microphone is shown in Fig. A.2. This frequency response function was derived from a transfer function measurement with a white noise electrical signal being applied to the coil of the driver.

CAPTIONS

Fig. 1 Nomenclature for measurement points.

Fig. 2(a) Magnitudes of the original (————) and the approximating (------) functions along the x axis.

(b) Gradients in the x, y and z directions of the original (————) and the approximating (------) functions along the x axis.

$L = M = N = 3$; $LL = MM = NN = 4$; $\ell = m = n = 1$.

Fig. 3(a) Magnitudes of the original (————) and the approximating (------) functions along the x axis.

(b) Gradients in the x, y and z directions of the original (————) and the approximating (------) functions along the x axis.

$L = M = N = 4$; $LL = MM = NN = 5$; $\ell = m = n = 1$.

Fig. 4(a) Magnitudes of the original (————) and the approximating (------) functions along the x axis.

(b) Gradients in the x, y and z directions of the original (————) and the approximating (------) functions along the x axis.

$L = M = N = 6$; $LL = MM = NN = 7$; $\ell = m = n = 2$.

Fig. 5(a) Magnitudes of the original (————) and the approximating (------) functions along the x axis.

(b) Gradients in the x, y and z directions of the original (————) and the approximating (------) functions along the x axis.

$L = M = N = 7$; $LL = MM = NN = 8$; $\ell = m = n = 2$.

Fig. 6 Enclosure used in experiments showing internal dimensions and axes orientation.

Fig. 7 (a) Pressure amplitude per unit volume velocity amplitude along the x axis from the measured values (•) and from the approximating function (———).

(b) Particle velocity amplitudes per unit volume velocity amplitude along the x axis.

$L = 4$, $M = N = 2$; $LL = 11$, $MM = 7$, $NN = 9$.

Fig. 8 (a) Pressure amplitude per unit volume velocity amplitude along the x axis from the measured values (•) and from the approximating function (———).

(b) Pressure amplitude per unit volume velocity amplitude along the y axis from the measured values (•) and from the approximating function (———).

(c) Particle velocity amplitudes per unit volume velocity amplitude along the x axis.

(d) Particle velocity amplitudes per unit volume velocity amplitude along the y axis.

$L = 7$, $M = 4$, $N = 2$; $LL = 11$, $MM = 7$, $NN = 9$.

Fig. A.1 Cross-section of calibrated volume velocity source.

Fig. A.2 Amplitude of frequency response curve for source.

Fig. 1 Nomenclature for measurement points.

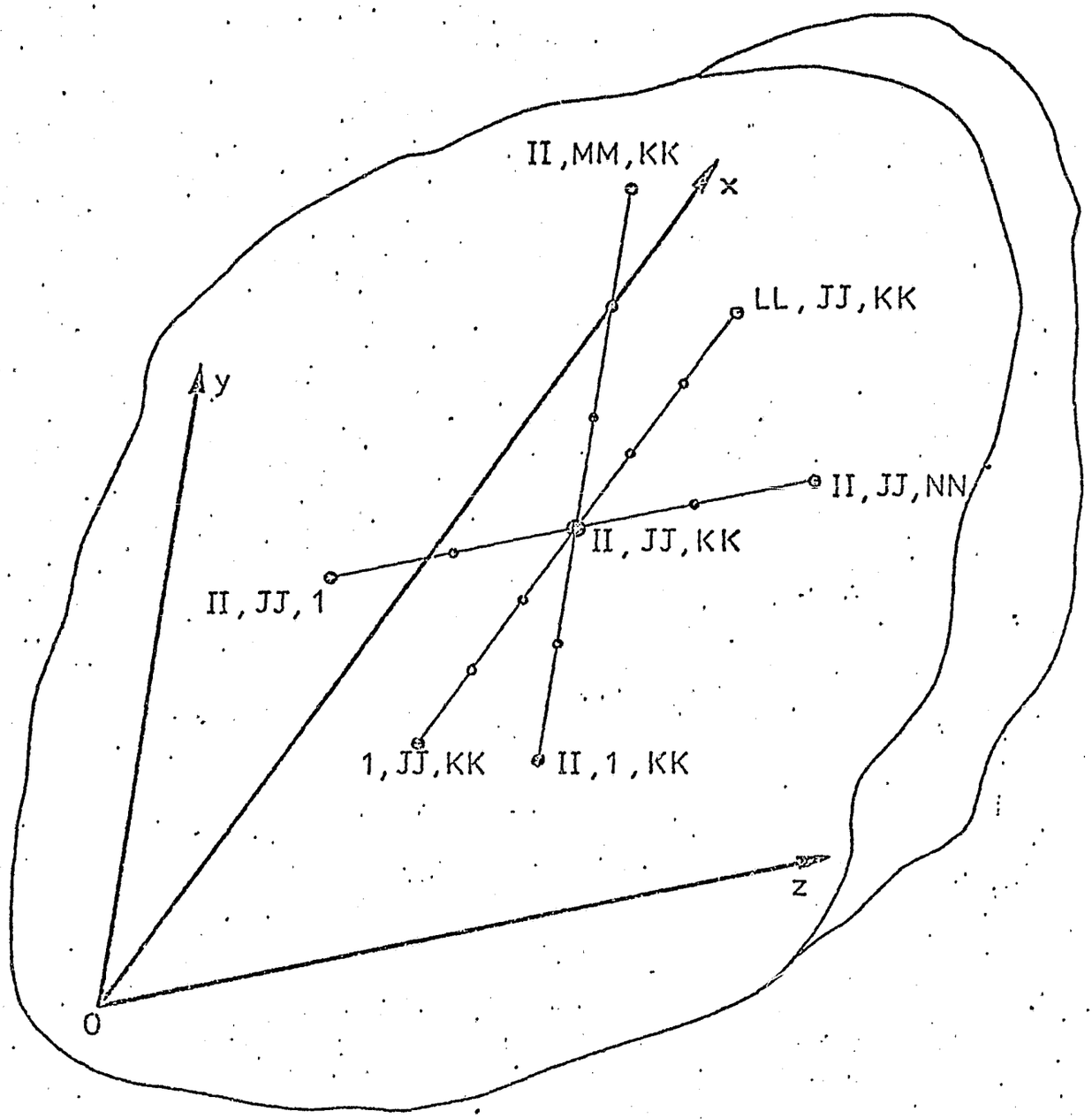

Fig. 2(a) Magnitudes of the original (———) and the approximating (------) functions along the x axis.

(b) Gradients in the x, y and z directions of the original (———) and the approximating (------) functions along the x axis.

L = M = N = 3 ; LL = MM = NN = 4 ; ℓ = m = n = 1 .

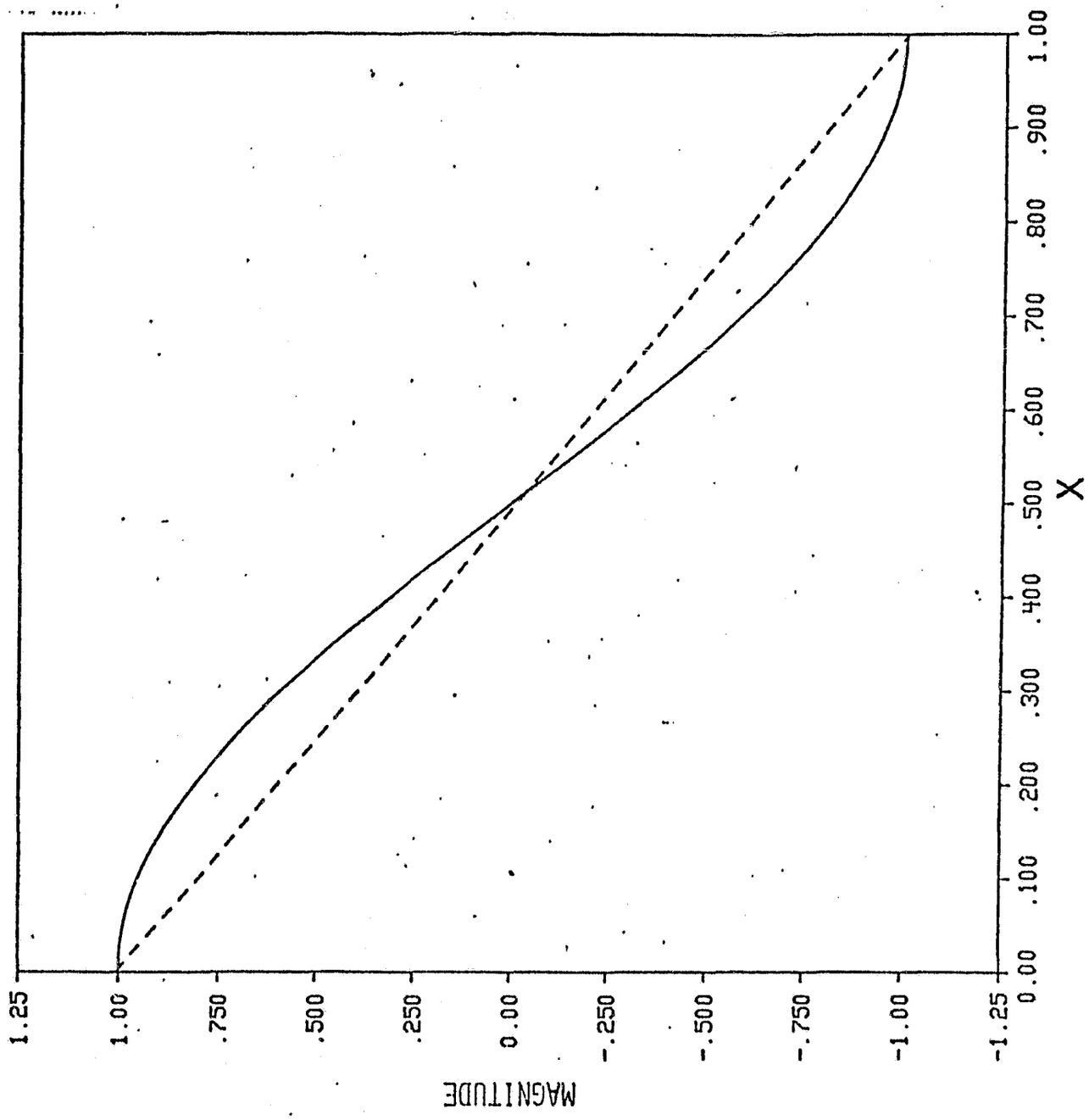

Fig. 2(a) Magnitudes of the original (———) and the approximating (------) functions along the x axis.

(b) Gradients in the x, y and z directions of the original (———) and the approximating (------) functions along the x axis.

L =M =N =3 ; LL =MM =NN =4 ; ℓ =m =n = 1 .

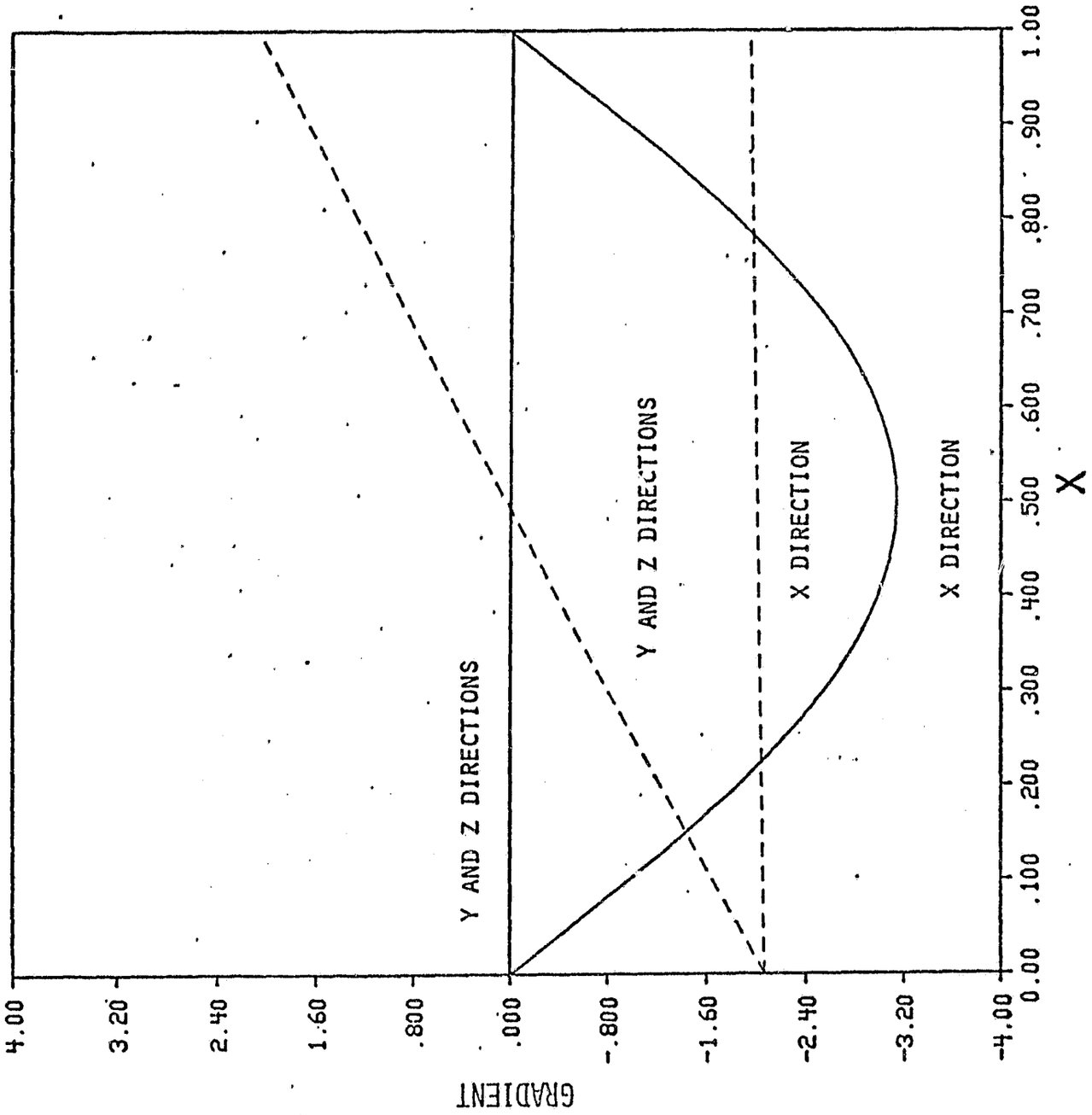

Fig. 3(a) Magnitudes of the original (———) and the approximating (-------) functions along the x axis.

(b) Gradients in the x, y and z directions of the original (———) and the approximating (-------) functions along the x axis.

L =M =N =4 ; LL =MM =NN =5 ; ℓ =m =n =1 .

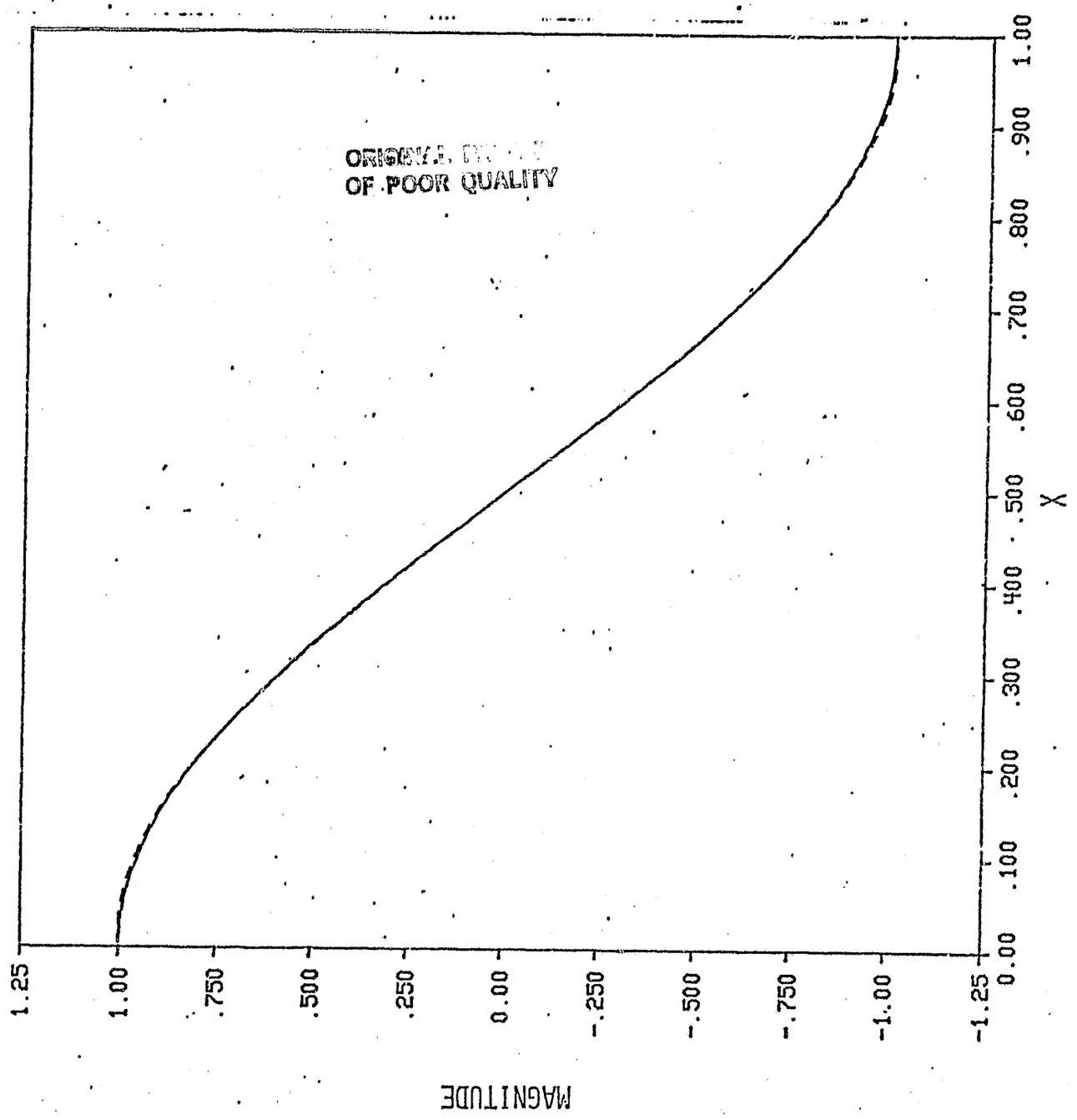

Fig. 3(a) Magnitudes of the original (———) and the approximating (-------) functions along the x axis.

(b) Gradients in the x, y and z directions of the original (———) and the approximating (-------) functions along the x axis.

L = M = N = 4 ; LL = MM = NN = 5 ; ℓ = m = n = 1 .

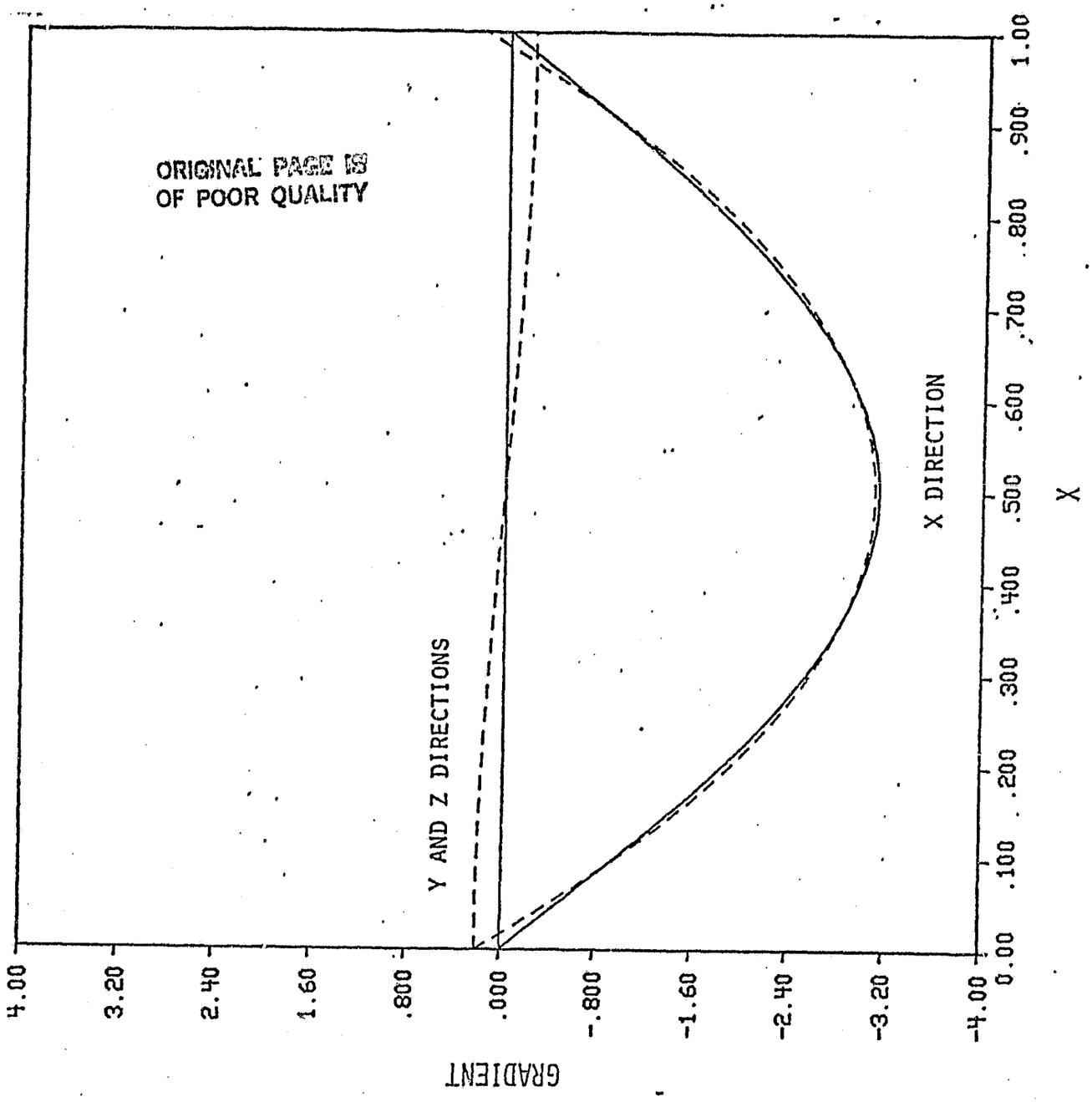

Fig. 4(a) Magnitudes of the original (———) and the approximating (- - - - - -) functions along the x axis.

(b) Gradients in the x, y and z directions of the original (———) and the approximating (- - - - - -) functions along the x axis.

L = M = N = 6 ; LL = MM = NN = 7 ; ℓ = m = n = 2 .

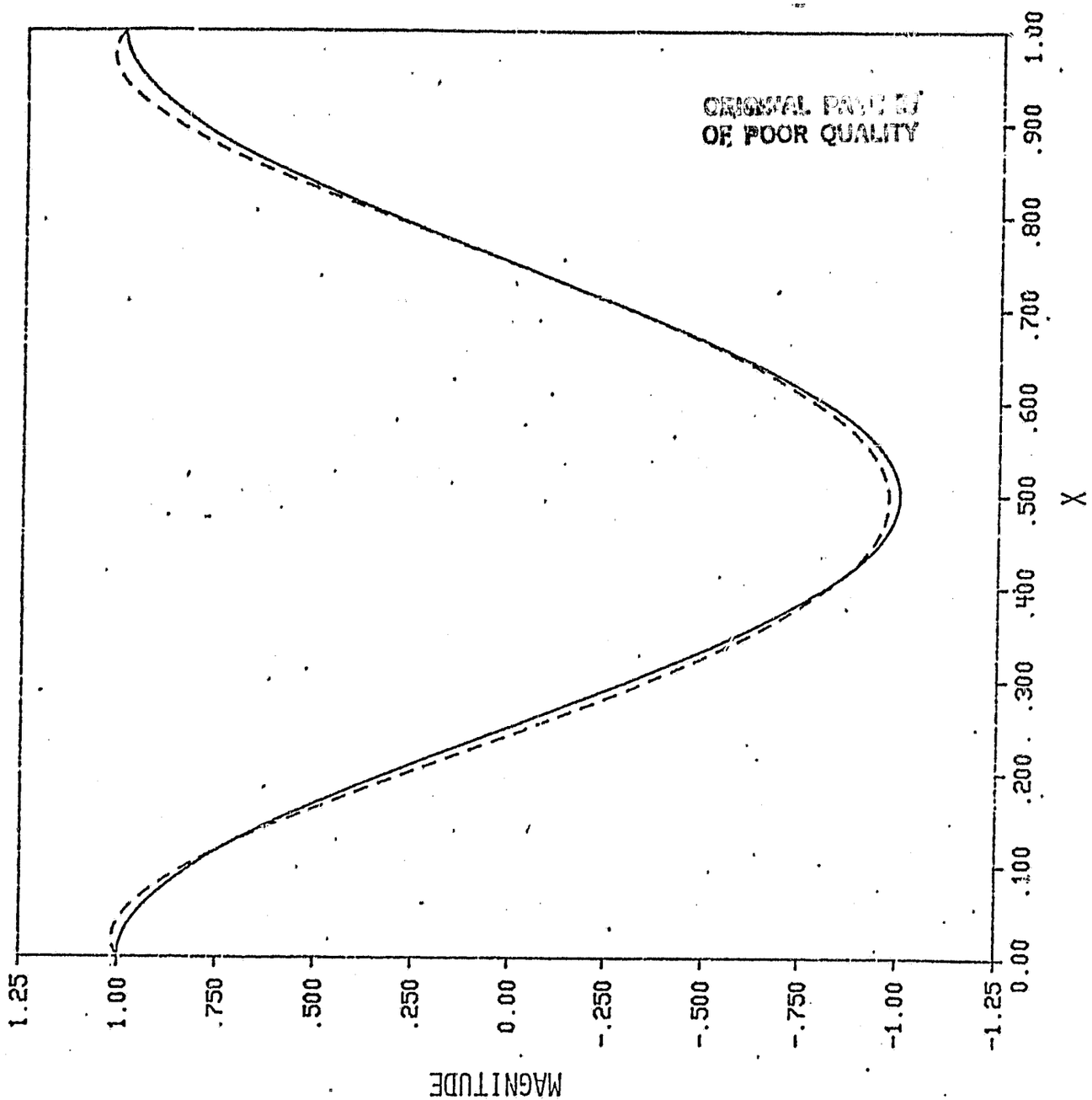

Fig. 4(a) Magnitudes of the original (———) and the approximating (- - - - - -) functions along the x axis.

(b) Gradients in the x, y and z directions of the original (———) and the approximating (- - - - - -) functions along the x axis.

L = M = N = 6 ; LL = MM = NN = 7 ; ℓ = m = n = 2 .

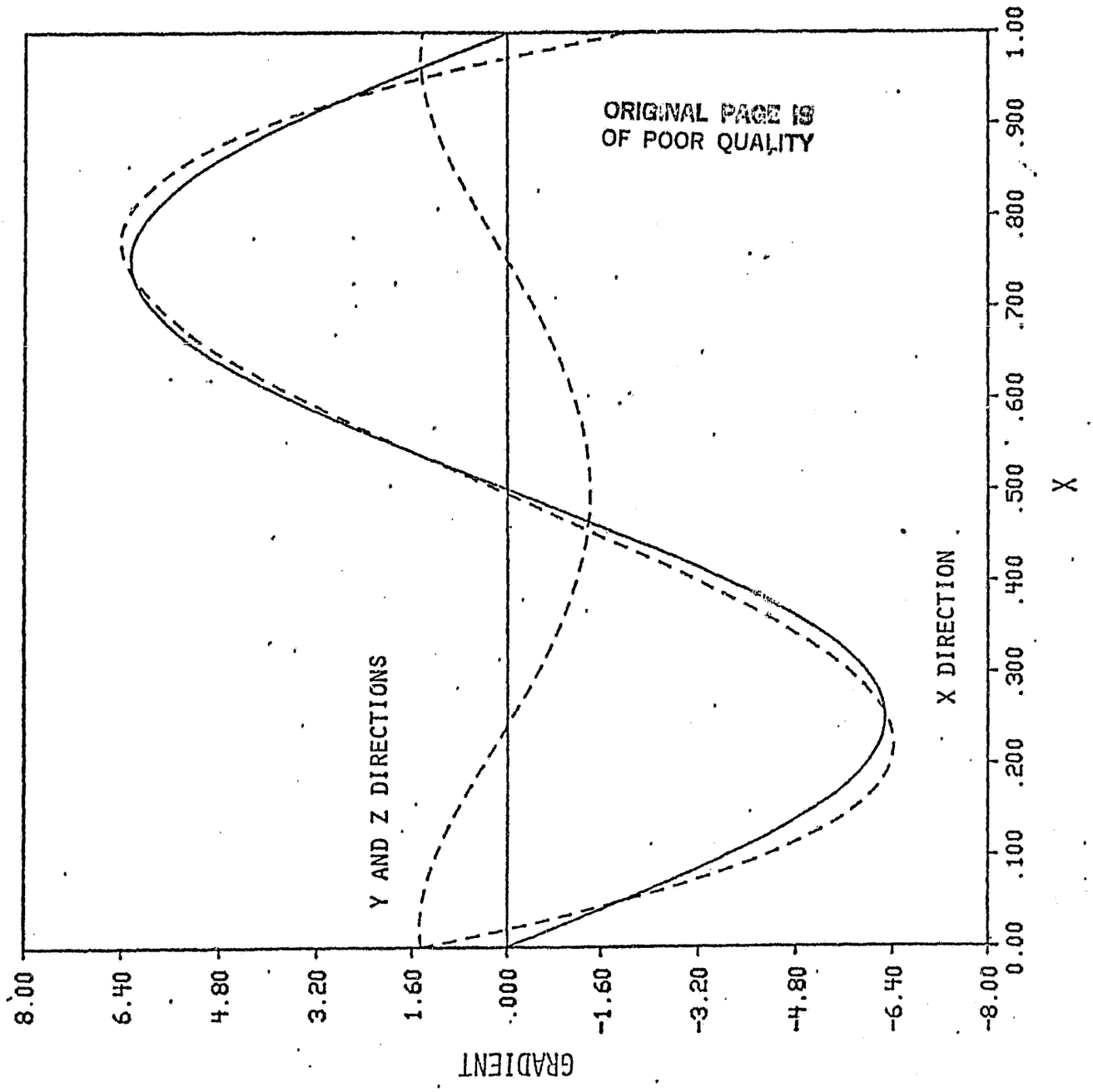

Fig. 5(a) Magnitudes of the original (———) and the approximating (-------) functions along the x axis.

(b) Gradients in the x, y and z directions of the original (———) and the approximating (-------) functions along the x axis.

L =M =N =7 ; LL =MM =NN =8 ; ℓ =m =n =2 .

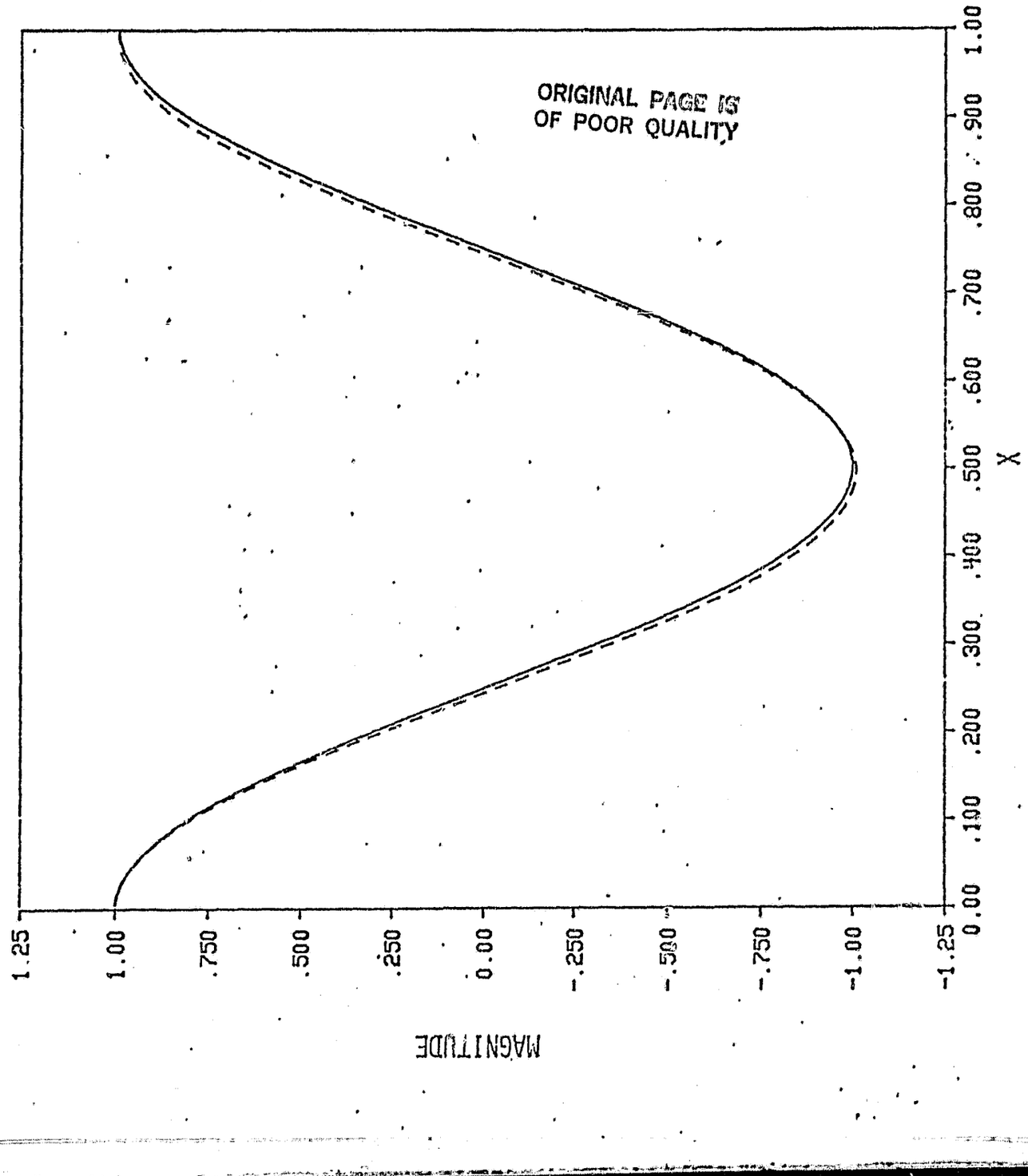

Fig. 5(a) Magnitudes of the original (———) and the approximating (– – – – –) functions along the x axis.

(b) Gradients in the x, y and z directions of the original (———) and the approximating (– – – – –) functions along the x axis.

L =M =N =7 ; LL =MM =NN =8 ; ℓ =m =n =2 .

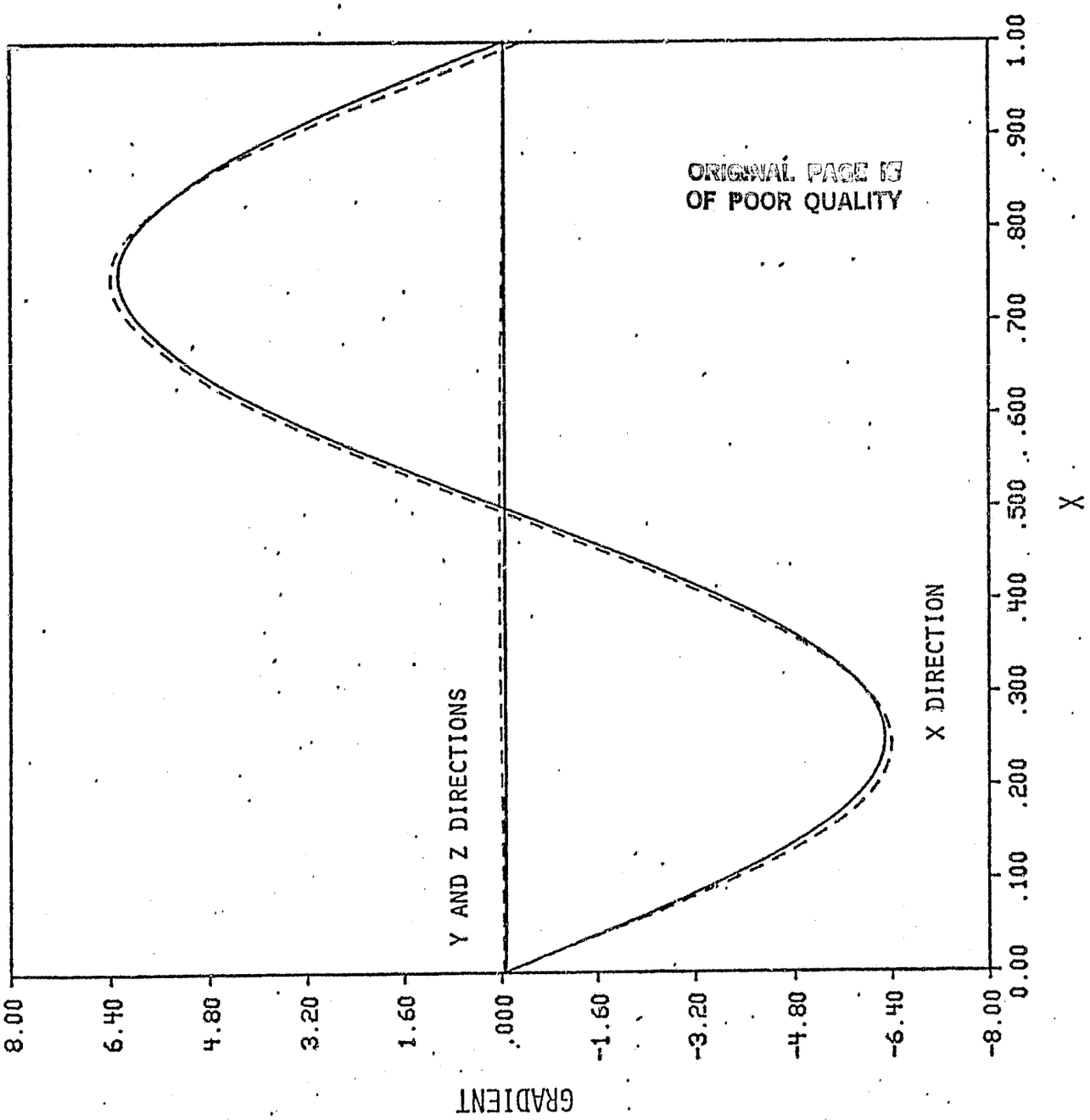

Fig. 6 Enclosure used in experiments showing internal dimensions and axes orientation.

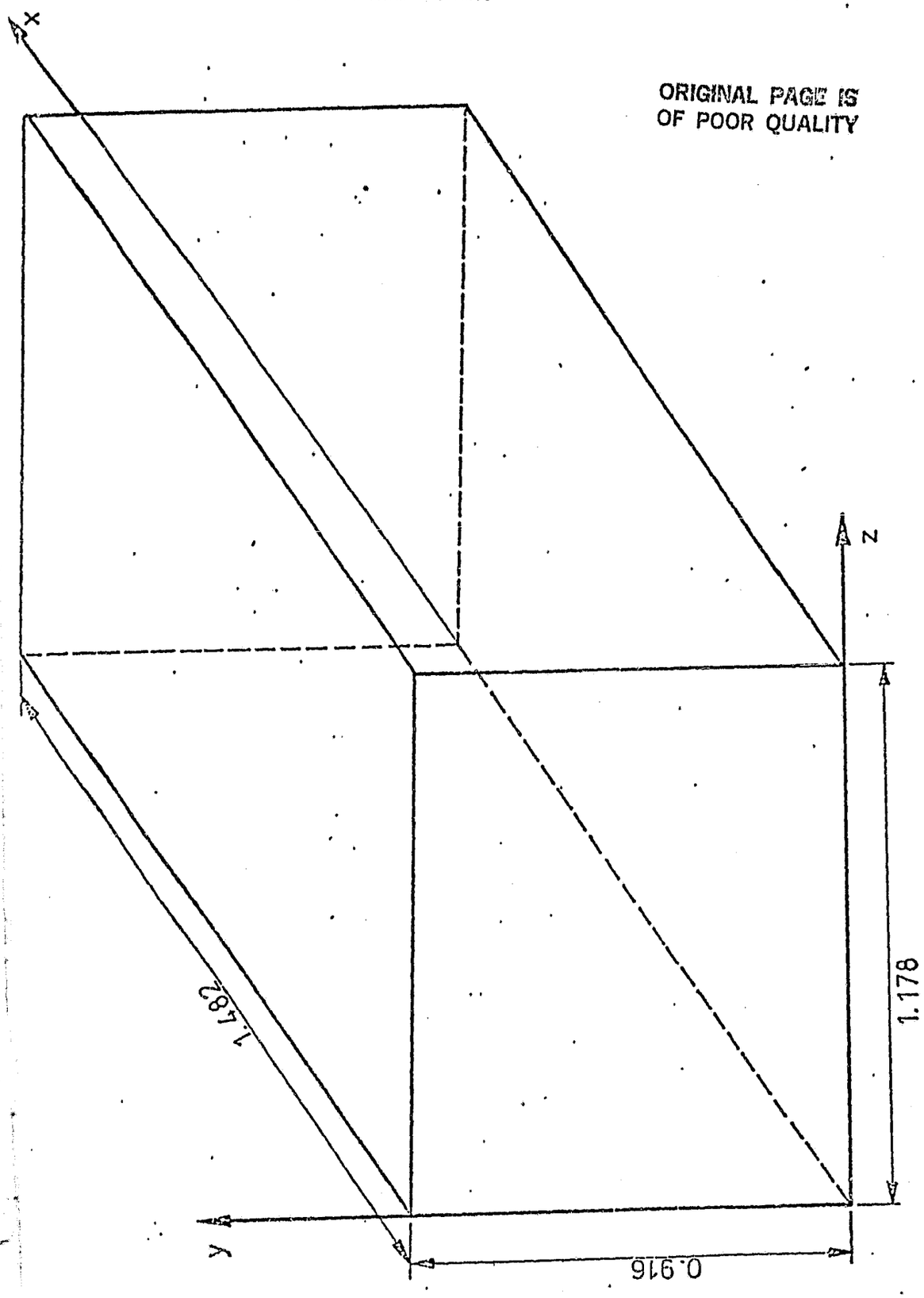

Fig. 7(a) Pressure amplitude per unit volume velocity amplitude along the x axis from the measured values (•) and from the approximating function (———).

(b) Particle velocity amplitudes per unit volume velocity amplitude along the x axis.

L =4 , M =N =2 ; LL =11 , MM =7 , NN =9 .

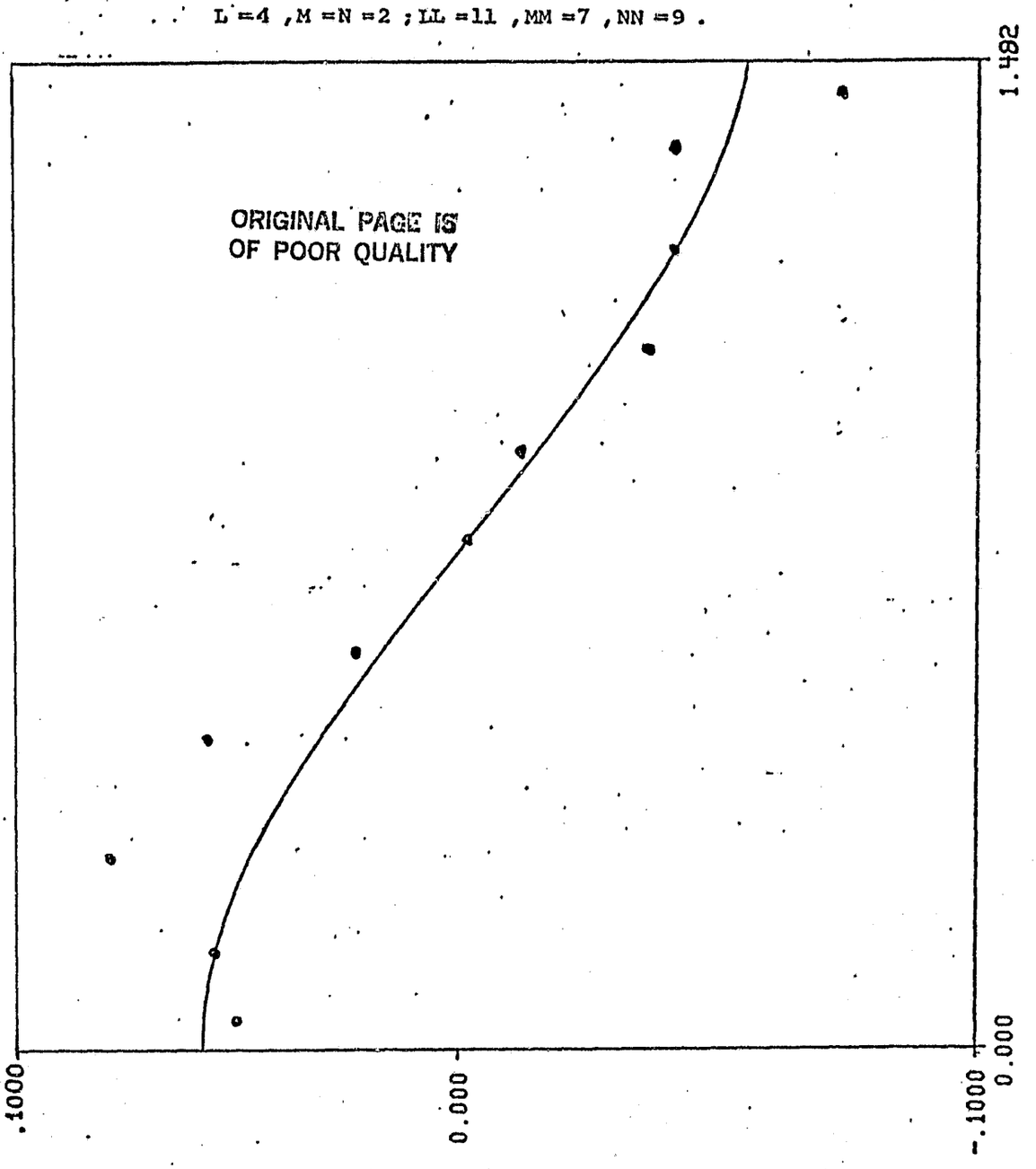

Fig. 7(a) Pressure amplitude per unit volume velocity amplitude along the x axis from the measured values (•) and from the approximating function (———).

(b) Particle velocity amplitudes per unit volume velocity amplitude along the x axis.

L =4 , M =N =2 ; LL =11 , MM =7 , NN =9 .

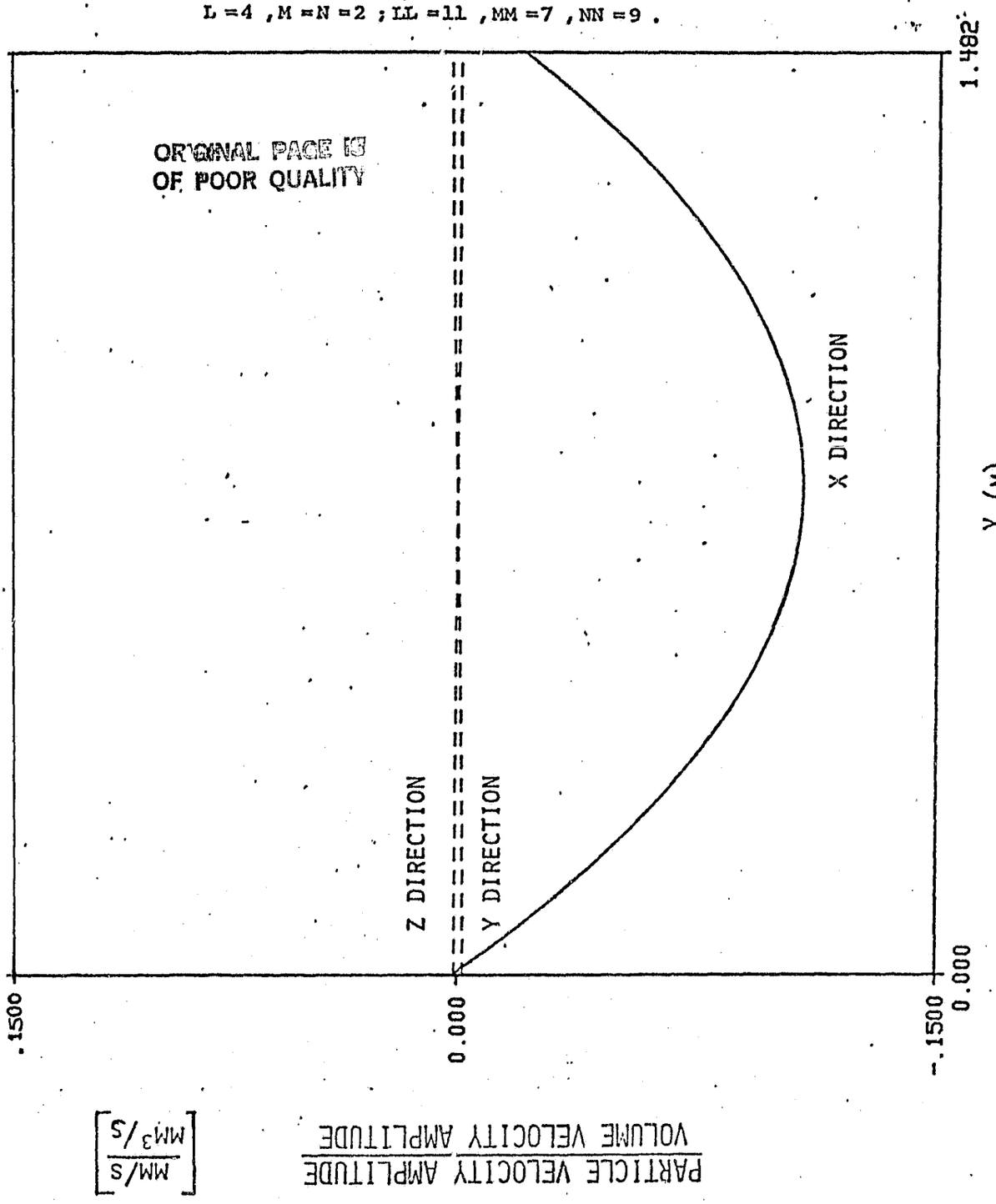

Fig. 8(a) Pressure amplitude per unit volume velocity amplitude along the x axis from the measured values (.) and from the approximating function ( ).

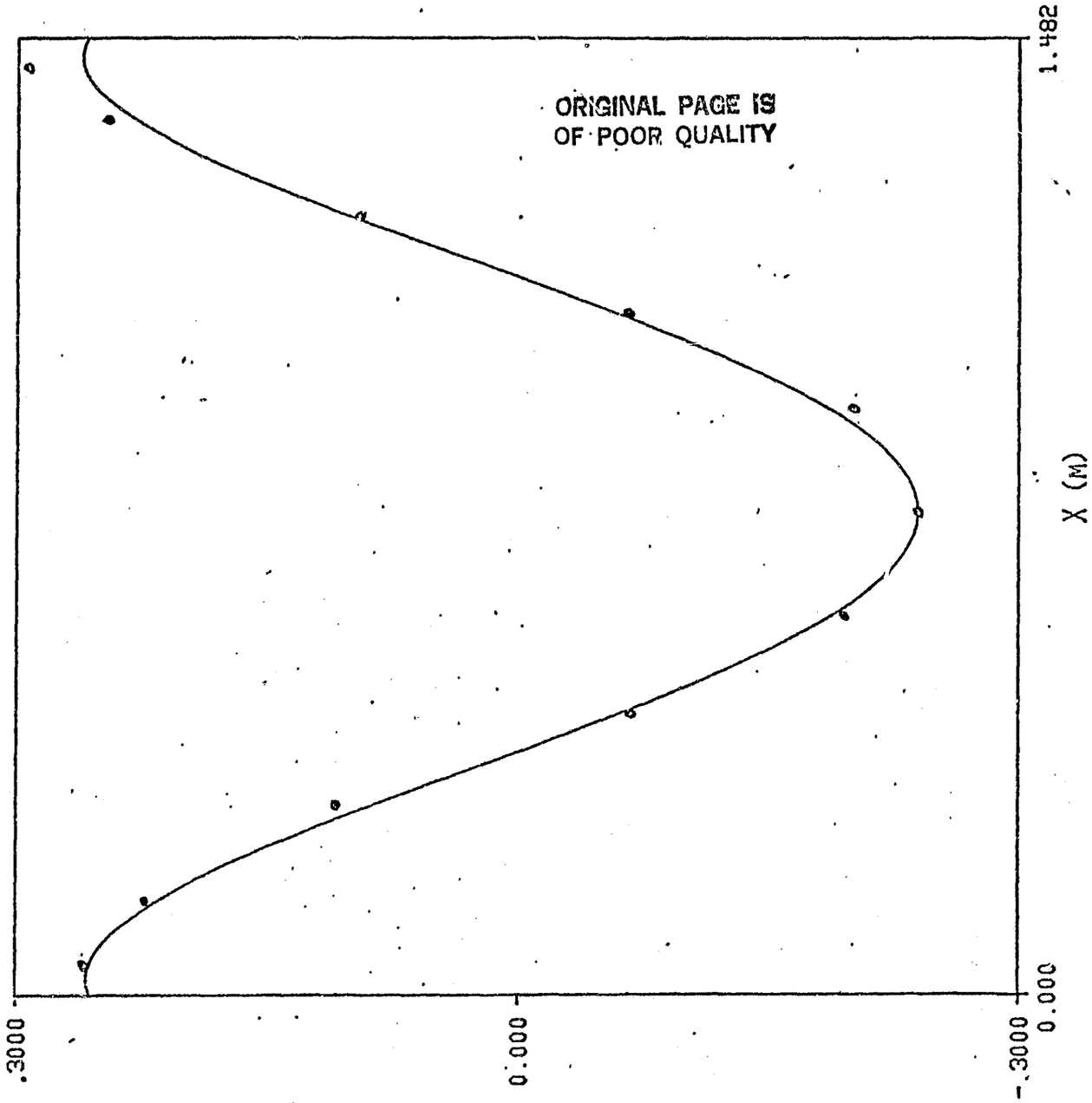

Fig. 8(b) Pressure amplitude per unit volume velocity amplitude along the y axis from the measured values (.) and from the approximating function( ).

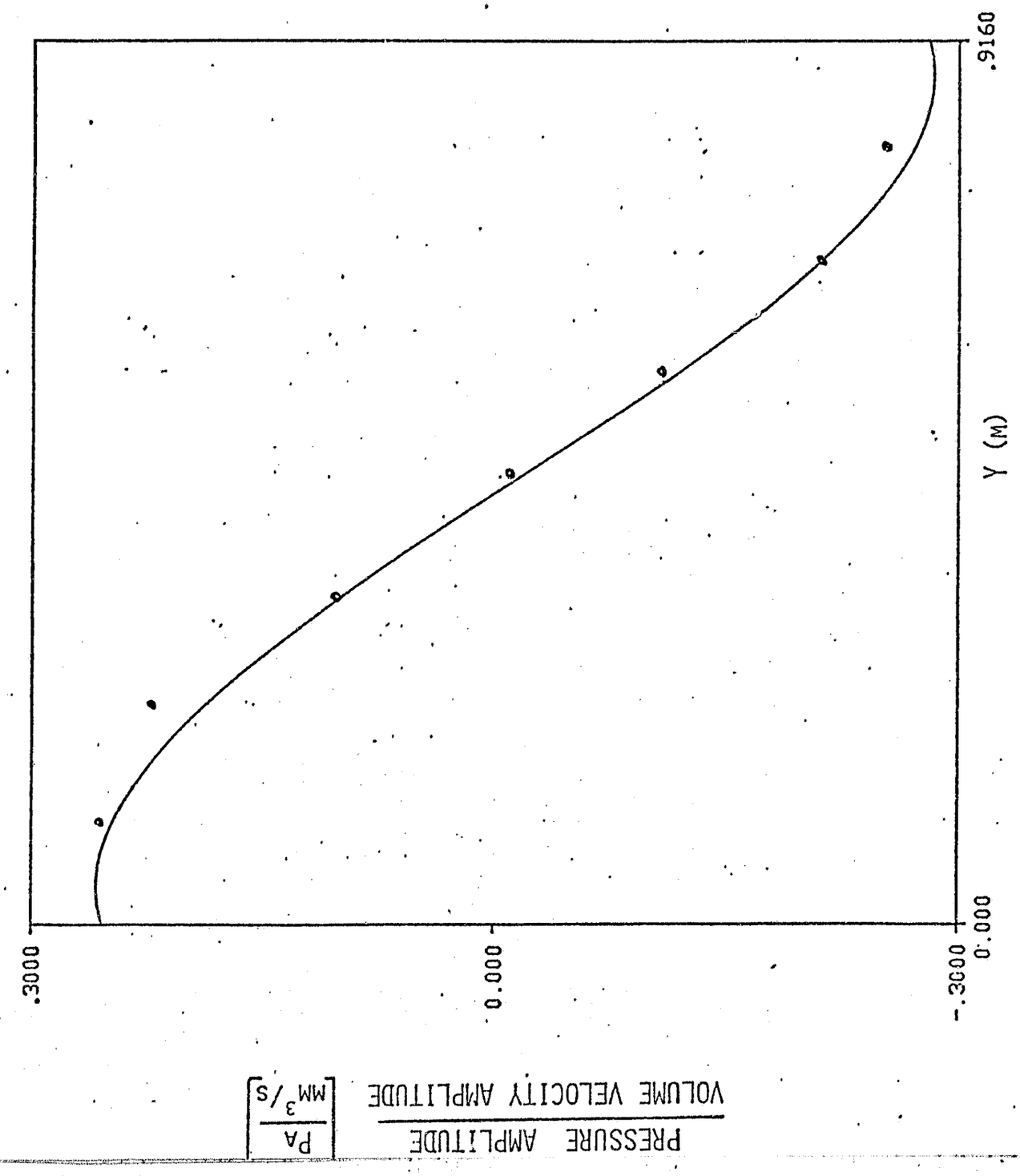

Fig. 8(c) Particle velocity amplitudes per unit volume velocity amplitude along the x axis.

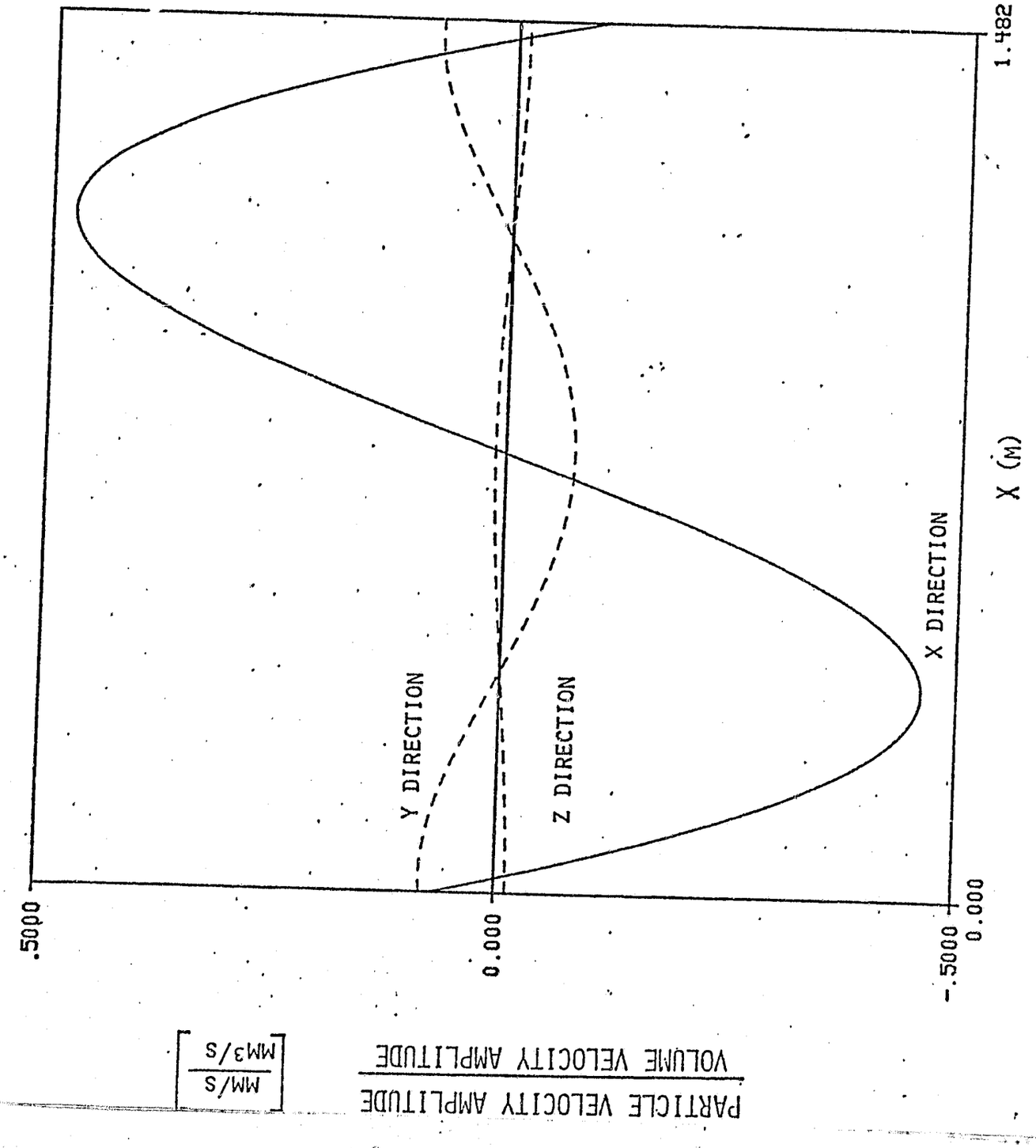

ORIGINAL PAGE IS
OF POOR QUALITY

Fig. 8(d) Particle velocity amplitudes per unit volume velocity amplitude along the y axis.

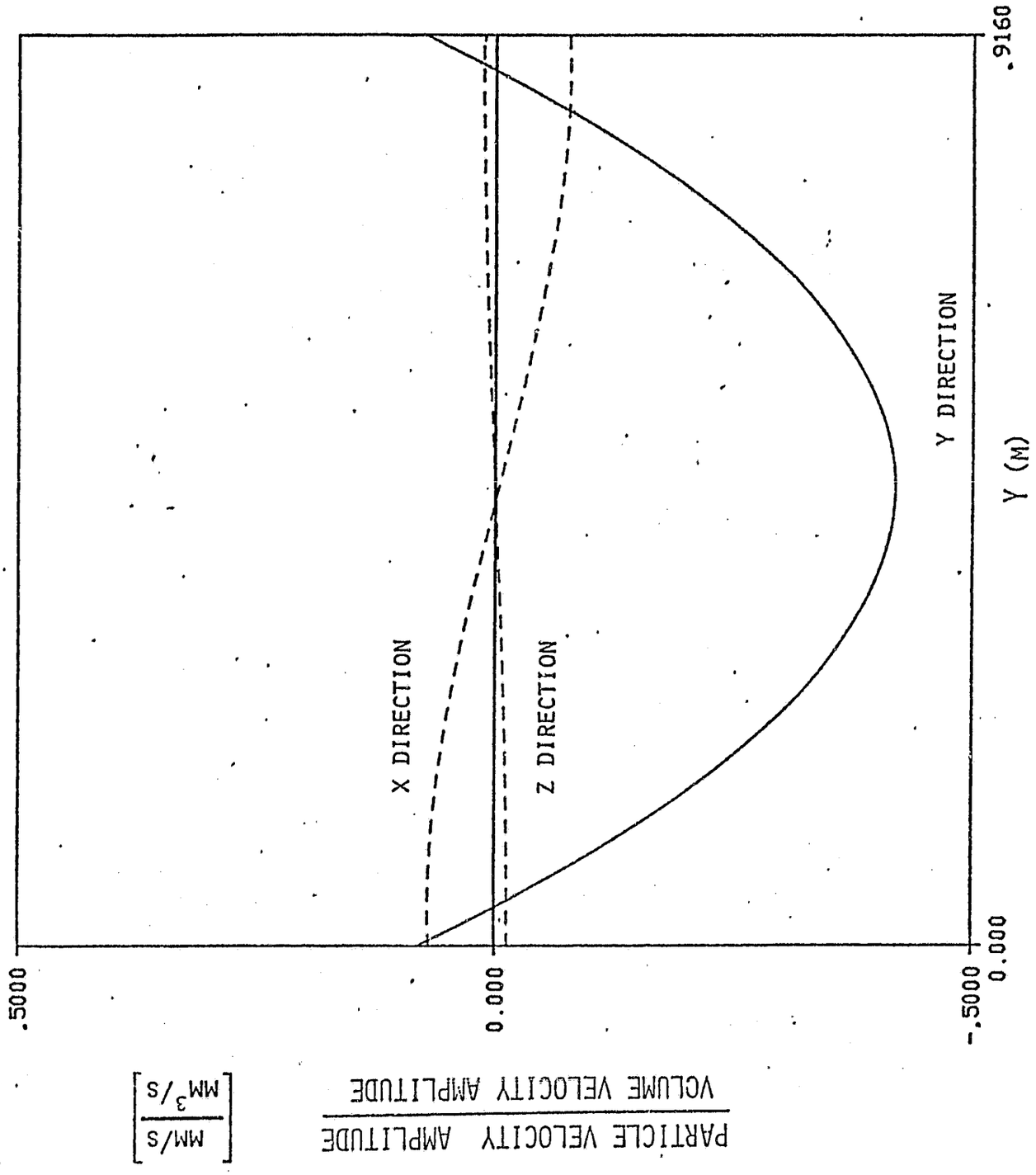

Fig. A.1 Cross-section of calibrated volume velocity source.

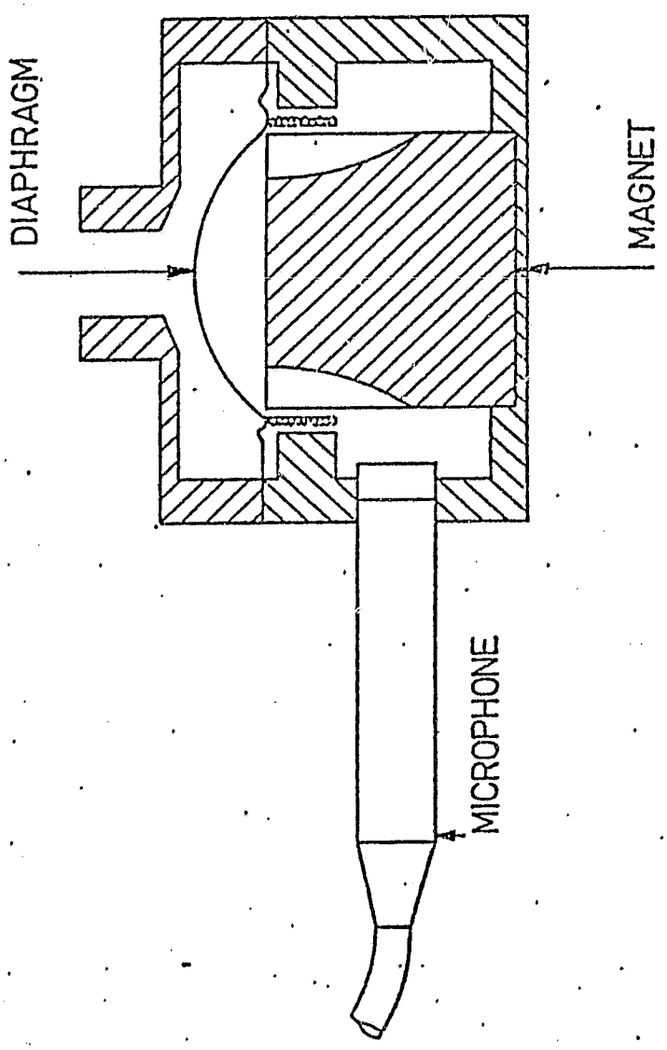

Fig. A.2 Amplitude of frequency response curve for source.